Bull. ERS, No.13 (1980)

NONLINEAR EARTHQUAKE RESPONSE OF EQUIPMENT SYSTEM ANCHORED ON R/C BUILDING FLOOR

by

Tsuneo OKADA[I], Koichi TAKANASHI[I],

Matsutaro SEKI[II] and Hidetake TANIGUCHI[II]

1. INTRODUCTION

The objective of this study was to investigate the influence of nonlinear behavior of support structure to the earthquake response of equipment structural systems installed on reinforced concrete buildings. For that purpose, an idealized structural system (Fig.1.1) was chosen and nonlinear response under severe earthquake condition was simulated by the IIS Computer-Actuator On-line System [1].

Existing equipment systems are of various kinds. The support structures of such systems have also wide varieties. Here an attempt was made to idealize such support structures into a simple comprehensive model structure. A equipment system supposed as a prototype is shown in Fig.1.1. The system is installed on the reinforced concrete floor of a building. The equipment itself is considered a only rigid mass for simplicity. The support structure consists of H-shaped steel columns, the tops of which are pinn-connected at the level where the center of gravity of the equipment mass exists. On the other hand, the bottoms of the columns are anchored on the floor.

The response behavior of this simple equipment system can be calculated by the following equation of motion:

$$M\ddot{x}_2 + C\dot{x}_2 + Q = -M(\ddot{x}_0 + \ddot{x}_1) \qquad (1.1)$$

where M : the mass of the equipment
C : the damping coefficient of the equipment system
Q : the restoring force
$\ddot{x}_0$: the ground acceleration at level C

I Associate Professor, Institute of Industrial Science, University of Tokyo
II Research Associate, Institute of Industrial Science, University of Tokyo

$\ddot{x}_1$: the floor acceleration at level B relative to level C

$\ddot{x}_2$: the equipment acceleration at level A relative to level B

$\dot{x}_2$: the equipment velocity at level A relative to level B

In Eq.(1.1), a coupling of the equipment system and the building system is not accounted directly, but the floor response of the building system is considered as an input to the equipment system.

If the support structure consists of columns with the same size, the response behavior of a single column boxed by dashed lines in Fig.1.1 can represent that of the whole system and calculated by a same equation as Eq.(1.1). Therefore, a column, fixed at the base, with the concentrated mass attached on the tip was analysed in the simulation described below.

The simulation is carried out twofold; firstly, cyclic load tests were done on predetermined column-top displacement loading program and secondly, load tests were conducted tracing the response displacements which were calculated simultaneously on the basis of restoring forces measured by the real-time procedure. The latter simulation system is called "IIS Computer-Actuator On-line System."

As to "On-line System", several papers have been already published [2,3,4,5,6]. Various kinds of simulations were also experienced. Here, the procedure of simulation is briefly explained. The flow diagram of the simulation is shown in Fig.1.2. Basically the main tasks are to solve Eq.(1.1) numerically by an approximate method, say, the linear acceleration method or the central difference method as the left flow in the figure, and to measure the instantaneous restoring force used in Eq.(1.1) experimentally by the computer-controlled load test on the very structure or structural model analysed as shown in the right flow of Fig.1.2. In the simulation described here a support column on the reinforced concrete footing was used as an analysis model. The mass of the equipment system concentrated on the tip of the column was determined so that desirable fundamental periods could be set. Input ground accelerations in this simulation should be the floor response accelerations of the reinforced concrete building.

2. TEST STRUCTURES AND TEST SETUP

2.1 Test Structures

The test structures investigated were canti-lever type columns fixed on the reinforced concrete thick slabs. In the tests, lateral loads were applied in the direction normal to the column

axes so that bending moment and shear force were produced at the column base. Test variables were the size, the embedment depth and the location arrangement of anchor bolts. As to the size, the rod diameters of all bolts were same as 22mmΦ, but the major thread diameter was specified as 27mmΦ for some of test structures which were distinguished by U in the specimen codes. The embedment depth was chosen to be 128mm and 208mm. These length-to-rod diameter ratios are 5.8 and 9.5 and designated by S and L in the code, respectively. The number of bolts was 4 or 6, which can be noticed in the code. The anchor head ring plates of 35mmΦ × 12mm, confirming to the Japanese Industrial Standards for studs, were welded to the bolts. The summary of test structures is in Table 2.1.

The H-shaped columns of the same size (H×150×150×7×10) and the same sized base plates (PL-300×300×12), which were attached to the bottoms of columns by shop-welding, were used for all specimens. The details of the test structures are shown in Fig.2.1. The details of reinforcement in the footing, the location and the sizes of reinforcement, are shown in Fig.2.1(c). To set the column bases at the proper position is rather difficult in experiment as well as in practical erection. In these test structures the satisfactory setting was achieved by use of a setting plate (PL-320×320×9) which was placed in its proper level when the concrete was casted. The setting plate worked also as a template to keep anchor bolts at their specified positions. After tightening the column to the concrete slab by nuts, the column base was welded to the setting plate.

2.2 Material Properties

The strength of steel, anchor bolt and concrete was measured by coupon tests on specified test specimens. The results are summarized in Table 2.2.

2.3 Test Setup

The test structures were fixed on the reaction wall in the laboratory by high tensile bolts as shown in Fig.2.2. Therefore, the load was applied to the column top by the hydraulic actuator (jack). The displacement of the actuator head was always controlled, according to the pre-determined displacement program in the cyclic tests and the simultaneously calculated response displacement in the on-line simulation.

2.4 Arrangement of Instrumentation

The load applied to the column top was measured electrically by the load cell mounted on the actuator head. The displacement of the column top denoted by X_2 was measured by the linear transformer. The uplift displacements of base plates were also measured by the linear transformers at the positions denoted by

D_2~D_5 in Fig.2.1. These data were converted into the digital form and recorded in magnetic tapes.

The strains at the surface of the base plate and the surfaces of column flanges near the base were obtained by electrical-resistance gages placed at the positions indicated by G1 to G8 in Fig.2.1. The elongations of anchor bolts were known by the strain results measured at the gages denoted as G9 G16. These strain data were used to examine the yielding of the parts and to know plastic deformation there.

3. CYCLIC LOADING TESTS

3.1 Loading Program

The cyclic load tests was carried out for four structural model specimens along the predetermined column-top displacement sequence. The loading programs are shown in Fig.3.1. For specimen (I-1-4S), one cycle static load test was done by the load control loading at the amplitude of 2.5tons. Then cyclic loading was continued in five cycles at the same amplitude. Thereafter, fifteen cycles were followed at the displacement amplitude of 3.0cm. As for specimen (II-1-4L), (IIU-1-4L) and (III-1-6L), the same procedure as (I-1-4S) was repeated till the amplitude of 3.0cm, but 5c., 10c. and 50c. cyclic tests were followed at the displacement amplitude of 5.0cm. One cycle static load test was preceded each cyclic test.

3.2 Test Results

The lateral load Q versus the displacement X_2 relationships at the tips of the column specimens (I-1-4S), (II-1-4L), (IIU-1-4L) and (III-1-6L) are shown in Fig.3.2(a) to (d). The maximum displacements X_{max} attained, the yield lateral load Q and the maximum Q_{max} observed in the tests are summarized in Table 2.1. The following descriptions of characteristic behavior must be added for each column specimen:

(1) I-1-4S (see Fig.3.2(a))

In the first cycle of loading the curve of Q vs. X_2 departs from a straight line beyond 1 ton, but no crack was found on the surface of the concrete slab. After the succeeding 5c. cyclic test, the cracks radiating in four directions from the anchor bolts were observed and the magnitude of Q decreased to 70~80% of the value attained at the first loading. The yielding appeared at around 2.0cm in the displacement of the column top. At the same time annular cracks could be noticed. That shows the tensile cracks beginning around the perimeters of anchor heads propagated to the footing surface. Another annular cracks appeared at further loading at the diaplacement of 3.0cm. The cracks developed and

sudden decrease in the lateral load took place in 15c. cyclic load test.

(2) II-1-4L (see Fig.3.2(b))
Stable loops in Q vs. X_2 can be observed till 12 cycle, though the loops were pinched due to plastic elongation of anchor bolts which caused uplifting of the column base. The yielding took place in 13 cycle. Any crack radiating from the anchor bolts and any annular crack were not observed.

(3) IIU-1-4L (see Fig.3.2(c))
In general the behavior was almost same as that of II-1-4L. The loads observed were slightly higher than those of II-1-4L at the same displacements. The reason is that the strength of concrete used in IIU-1-4L was higher and the yield strength of anchor bolts was also higher, because in this specimen the so-called upset bolts were used, in which the stress area of threaded part was greater than the nominal area of the rod. No crack caused by concrete tensile failure was observed.

(4) II-1-6L (see Fig.3.2(d))
The most stable loops were obtained, although these are pinched. The pinched loops resulted partly from the uplift of anchor nuts due to plastic deformation of bolts. One of the measured uplift displacements is shown in Fig.3.3. A few cracks radiating from the anchor bolts were observed. The yielding of the column itself was considered to occur by the results of strain measurement of the flange surface near column base.

4. ON-LINE TESTS

4.1 Test Variables

In the simulations by "IIS Computer-Actuator On-line System" the natural period of an assumed equipment system and the intesity of an input acceleration can be arbitrarily determined in reference to the stiffness and the strength of a test structure.

(1) Natural period
The period of the fictitious building is 0.4 sec as described later. Then, two periods of 0.8 sec and 0.3 sec were considered in order to interpose 0.4 sec between them. The period of 0.8 sec was assigned to the first group of I-2-4S III-2-6L and the period of 0.3 sec to the second group of IU-3-4S IIIU-3-6L as shown in Tables 2.1 and 4.1. The fictitious mass on the tip of a support column was automatically calculated using the stiffness and the assigned period. The stiffness K_0 used is defined as the amount of the lateral load required for an unit displacement normal to the column axis at the top. The displacement is mainly due to the bending of the steel column, but the effect of the shear

deformation of the web plate is considered. The loss of the stiffness caused by the elastic deformation in the bolts and the slab is not taken in the stiffness calculation. As shown in Table 4.1, the periods based on the measured stiffness are different from the nominal K_0. The calculation results are summarized in Table 4.1.

(2) Input acceleration

The input acceleration used in the simulation must be the floor acceleration. It was assigned the elastic response acceleration of a single story building with the period of 0.4 sec and the dumping ratio of 2 % to the EW component of HACHINOHE record in 1968 TOKACHI-OKI earthquake. The time history is shown in Fig.4.1. The acceleration response spectrum is shown in Fig.4.2.
The maximum acceleration $(\ddot{x}_0 + \ddot{x}_1)_{max}$ was determined as

$$(\ddot{x}_0 + \ddot{x}_1)_{max} = Q_{Y0}/(\alpha_0 M) \qquad (4.1)$$

where Q_{Y0} = the full plastic moment of the column/L
L = the length of the column
M = the mass assumed

The arbitrary coefficient α_0 was set 1.87 in the simulation. The same value of α_0 was used for all specimens in order to examine how the response behaviors of the equipment systems are influenced by the deterioration of stiffness and strength at column bases and /or anchorages.

4.2 Test Results

Some of response displacement time histories are shown in Fig.4.3. In the response displacements of the first group with the nominal period of 0.8 sec, namely I-2-4S, II-2-4L, IIU-2-4L and III-2-6L, the maximum response displacement occurred in 5～7 sec and the response periods were estimated 1.3 sec approximately in the vicinity of the maximum. Thereafter the response gradually damped. Especially in II-2-4L and IIU-2-4L the rapid damping was observed. This tendency can be understood from the viewpoint of the response spectrum. The plastic deformation in the anchorage had the response periods prolonged. In consequence, the response decreased and the severe damage was avoided.

On the other hand the large response took place in the second group with the nominal period of 0.3 sec. In the response of IU-3-4S the maximum value occurred in 4.8 sec and the observed period was about 0.6 sec. In further response the failure in the reinforced concrete footing advanced and the strength was much reduced. The complete failure was observed in the result.

The response behaviors of II-3-4L and IIU-3-4L were almost same. The large response displacement peaks appeared twice in

2 sec and 5.8 sec. The response periods were 0.4 sec and 0.5 sec near the peaks, respectively. The response became smaller after the second large peak, but the considerable residual displacements was observed.

There is a slight difference in the response time histories of Ⅲ-3-6L and ⅢU-3-6L. The histories are almost same till 3.5 sec. The maximum response was recorded in 3.35 sec in Ⅲ-3-6L, but it was recorded in 5.78 sec in ⅢU-3-6L. After 8 sec the histories are almost same again. The residual displacement was observed in both specimens.

The response shear force-displacement diagrams are shown in Fig.4.4. In the figures the values of yield strength Q_Y observed are also indicated.

5. FAILURE MECHANISM AND ULTIMATE STRENGTH OF SUPPORT STRUCTURES

5.1 Failure Mechanism

Failure mechanisms observed in the test were;

(1) Pull out failure of slab concrete (Type S)
(2) Yielding in tension of anchor bolts (Type B)
(3) Yielding in bending of H-shaped column (Type H)
(4) Bearing failure of concrete at anchor head (Type C)

However, the bearing failure was not predominated, but associated with the flexural yielding of H-shaped column.

(1) Pull out failure of slab concrete (Type S) was observed in the specimens-4S. As shown in Fig.5.1, tensile failure occurred on the surface of stress corn inclined about 45° to the slab surface. Radial splitting tensile cracks were also observed on the slab surface shown in Fig.5.2.

(2) Yielding in tension of anchor bolts (Type B) was observed in the specimens-4L. In the case of standard type of bolts, yielding occurred at threaded part first, then, rod part yielded, while threaded part did not yield in upset bolts. Crack was not observed on the slab surface, except minor flexural cracks.

(3) Yielding in bending of H-shaped column (Type H) was observed in the specimens-6L which was anchored most firmly. Neither yielding of anchor bolts nor pull out failure occurred. However, radial splitting tensile cracks were observed. After the test, inside crack around bolts was examined by core boring, then, pull out crack and minor bearing failure of concrete at the anchor head were found.

Among their failure types, the pull out failure (Type S) was most brittle and the bending yielding type of H-shaped column was most ductile.

5.2 Calculation of Yield Strength

Yield strength for each failure type was calculated by a full plastic theory. Analytical model and stress distribution are shown in Figs.5.3(a) and (b). Assumption in the calculation are;

a) Base plate is rigid,
b) Stress-strain relationships of concrete both in tension and compression and anchor bolts are rigid-plastic,
c) Anchor bolt does not work in compression,
d) When one type of failure is predominated, other types of failure do not occur, and
e) Shape factors of concrete stress block (k_1 ,k_2 ,k_3) are; k_1 =0.85, k_2=k_1/2, k_3=0.85 [7].

(1) Strength at pull out failure of slab concrete;

Tensile force of anchor bolt when the pull out failure occurred first, T_S, was calculated by Eq.(5.1).

$$T_S = f_S \, A \tag{5.1}$$

where f_S : tensile strength of concrete (kg/cm^2).
A : projected area of concrete stress corn (see Fig.5.4)

For the tensile strength of concrete, $1.1\sqrt{f_c}$ and f_t were used, where f_c is concrete compressive strength in kg/cm^2 and f_t is concrete splitting tensile strength. Lateral load working at the top of the H-shaped column, P_S, was calculated by Eq.(5.2).

$$P_S = T_S \, j/L \tag{5.2}$$

where j : distance between the bolt and the center of concrete stress block calculated by the full plastic theory.
L : distance between the bottom of base plate and the lateral loading point

(2) Strength at yielding in tension of anchor bolts;

Lateral load when the anchor bolts yielded first, P_B, was calculated by Eq.(5.3).

$$P_B = T_B \, j/L \tag{5.3}$$

where T_B : sum of yield strength of bolts in tension.

(3) Strength at bearing failure of concrete at anchor head;

Lateral load when the concrete at anchor head crushed locally, P_C , was calculated by Eq.(5.4)

$$P_C = f_c \sqrt{\frac{A}{A_1}} A_1 \, j/L \tag{5.4}$$

where A : projected area of concrete stress corn (see Fig.5.4)
A_1 : bearing area at anchor head

Ultimate strength for yielding of H-shaped column was calculated by full plastic moment concept.

5.3 Relation between Failure Mechanism and Strength

(1) Yield strength:
Calculated yield strength and observed one in the tests were compared in Table 5.1, Figs.5.5 and 5.6. As seen in the table and the figures, the calculated values showed a good agreement with the observed value. The discrepancy between them was within 20%. For each specimen, the failure mode having the smallest strength among the calculated strength corresponding to failure types controlled the failure mechanism in the test.

(2) Ultimate strength:
Ratio of ultimate strength to yield strength in the test was shown in Table 5.1. When the pull out failure occurred, the ratio was almost unity. In other word, the increase of lateral load after yielding was not observed. As for other types of failure mode, 10～30% of strength increase was observed according to the increase of deformation after yielding.

6. EARTHQUAKE RESPONSE OF EQUIPMENT SYSTEM

6.1 Elastic Stiffness and Natural Period

As previously described, the stiffness K measured in the obtained response shear force-displacement diagrams result in the smaller values, say, 56～74% of the nominal values K_0 . The reason is that the nominal values K_0 were calculated on the basis of the stiffnesses of H-shaped steel support columns. Therefore, the pull-out of the anchor bolts and the bending of the base plates were not considered in the calculations.

The initial natural periods T of the assumed equipment systems with these support columns are summarized in Table 4.1. These become the longer periods in comparison with the corresponding nominal periods. Namely, the periods of the systems with 0.8 sec assigned vary between 0.95 sec and 1.04 sec, and the periods of the systems with 0.3 vary between 0.35 sec and 0.41 sec.

As for the response periods observed along the time histories of response displacements the discussions were already done in the previous article. It is worth to be noted that the nominal periods from the nominal stiffnesses are quite different from those observed in the simulation.

6.2 Response Shear Forces and Displacements

The response shear force-displacement relationships are shown in Fig.4.4. In general these are the same sort of curves as those obtained in the cyclic tests. The maximum values of the response displacements and shear forces are summarized in Table 4.1. These are also expressed in the non-dimensional forms, where the observed values of yield displacements x_Y and the observed yield shear forces Q_Y are used. Apparently some of the response shear forces cannot reach the yield strength before failure. For instance, IU-3-4S shows nearly 0.6 in Q_{max}/Q_Y, II-3-4L and II U-3-4L show 1.0, and III-3-6L and II U-3-4L show 1.3.

In Fig.6.1 the elastic-plastic response spectra of column-top displacement is shown, where a bi-linear type restoring force characteristics model with 2% of elastic stiffness after yielding are adopted and the following equation in the non-dimensional form was used in the calculation:

In the elastic range,

$$\ddot{\mu} + \omega_o^2 \mu = -\frac{1}{\alpha}\omega_o^2 \ddot{\zeta} \qquad (6.1)$$

where $\mu = x/x_Y$
$\omega_o^2 = k/M$
$\alpha = Q_Y/M(\ddot{y}_{max})$
$\ddot{\zeta} = \ddot{y}/\ddot{y}_{max}$
x = response displacement
$\ddot{y}$ = input acceleration

In the plastic range,

$$\ddot{\mu} + \omega_o^2 f = -\frac{1}{\alpha}\omega_o^2 \ddot{\zeta} \qquad (6.2)$$

where $f = Q/Q_y$

In spite that the same value, 1.87, was assigned to α_o for all specimens (see 4.1(2)) the real values α result in the different values since the observed yield strength Q_Y are different from the nominal yield strength Q_{Yo}. The values α are listed in the last column of Table 4.1. Being aware of these values, the test results plotted in the figure can be compared with the spectrum curves. It is clear that almost all test results are larger than the corresponding spectrum curves. Such tendency was significant in the specimens failed by tensile fracture of concrete (Specimens-4S). Even though concrete slab did not fail, the same tendency was observed, because of the pinched force-displacement curves due to plastic deformation in anchor bolts.

7. CONCLUDING REMARKS

The concluding remarks obtained by the simulations are summarized as follows:

(1) Earthquake response of equipment systems installed on reinforced concrete building is influenced sensitively the arrangement, the embedment depth and the threaded part deformation which control the failure mechanism of anchorage.

(2) The expected failure mechanisms are
a) Pull out failure of slab concrete
b) Yielding in tension of anchor bolts
c) Yielding in bending of H-shaped column
d) Bearing failure of concrete at anchor head
In the test, one of the mechanisms (a),(b) and (c) was dominated depending on the anchorage type. The combination of (a),(b) and (c) was also observed. But the mechanism (d) was not significant. Pull out failure should be avoided in the structural design, since it will cause the extremely brittle failure under earthquake condition.

(3) The calculation based on the full plastic concept could predict well the strength and the corresponding failure mechanism.

(4) The deformation of anchor bolts and base plates must be considered in calculating the elastic stiffness of the system.

(5) For practical design purpose, analytical models representing the complicating restoring force characteristics observed in the test should be developed, which are left for further studies.

(6) It is verified that IIS Computer-Actuator On-line System is applicable for simulation of earthquake response of the complex system by connecting the specific behavior of subsystems; equipment, support structure and building structure.

ACKNOWLEDGEMENTS

The authors acknowledge with gratitute the finantial support and valuable advices of EDR Research Group which made this work possible. Also, they wish to express their thanks to Messrs. Y. Shimawaki, K. Okada, K. Yamaguchi, H. Kondo and M. Teshigawara for cooperation in conducting the tests.

REFERENCES

[1] TAKANASHI,K., UDAGAWA,K., SEKI,M., OKADA,T. and TANAKA,H., "Non-linear Earthquake Response Analysis of Structures by a Computer-Actuator On-line System," Bulletin of ERS, No.8, Dec. 1974.

[2] OKADA,T. and SEKI,M., "A Simulation of Earthquake Response of Reinforced Concrete Buildings," Proc. of 6-WCEE, New Delhi, India, Jan. 1977.

[3] TAKANASHI,K., UDAGAWA,K. and TANAKA,H., "A Simulation of Earthquake Response of Steel Buildings," Proc. of 6-WCEE, New Delhi, India, Jan. 1977.

[4] OKADA,T., "The Experimental Investigation on ERCBC with Emphasis on the use of Earthquake Response Simulators in Japan," Proc. of Workshop on Earthquake-Resistant Reinforced Concrete Building Construction (ERCBC)," University Extension, Univ. of California, Berkeley, Ca. U.S.A., July 1977.

[5] OKADA,T., SEKI,M. and PARK,Y.J., "A Simulation of Earthquake Response of Reinforced Concrete Building Frames to Bi-directional Ground Motion by IIS Computer-Actuator On-line System," A Paper submitted to 7-WCEE, Istanbul, Turkey, Sept. 1980.

[6] TAKANASHI,K., UDAGAWA,K. and TANAKA,H., "Pseudo-Dynamic Tests on a 2-story Steel Frame by Computer-Load Test Apparatus Hybrid System," A Paper submitted to 7-WCEE, Istanbul, Turkey, Sept. 1980.

[7] AMERICAN CONCRETE INSTITUTE, "Building Code Requirements for Reinforced Concrete"(ACI 318-77). (Manuscript was received on March 31, 1980)

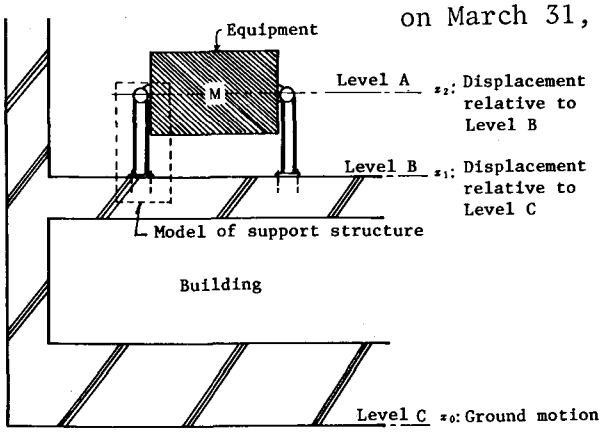

Fig.1.1 The equipment system assumed in the simulations

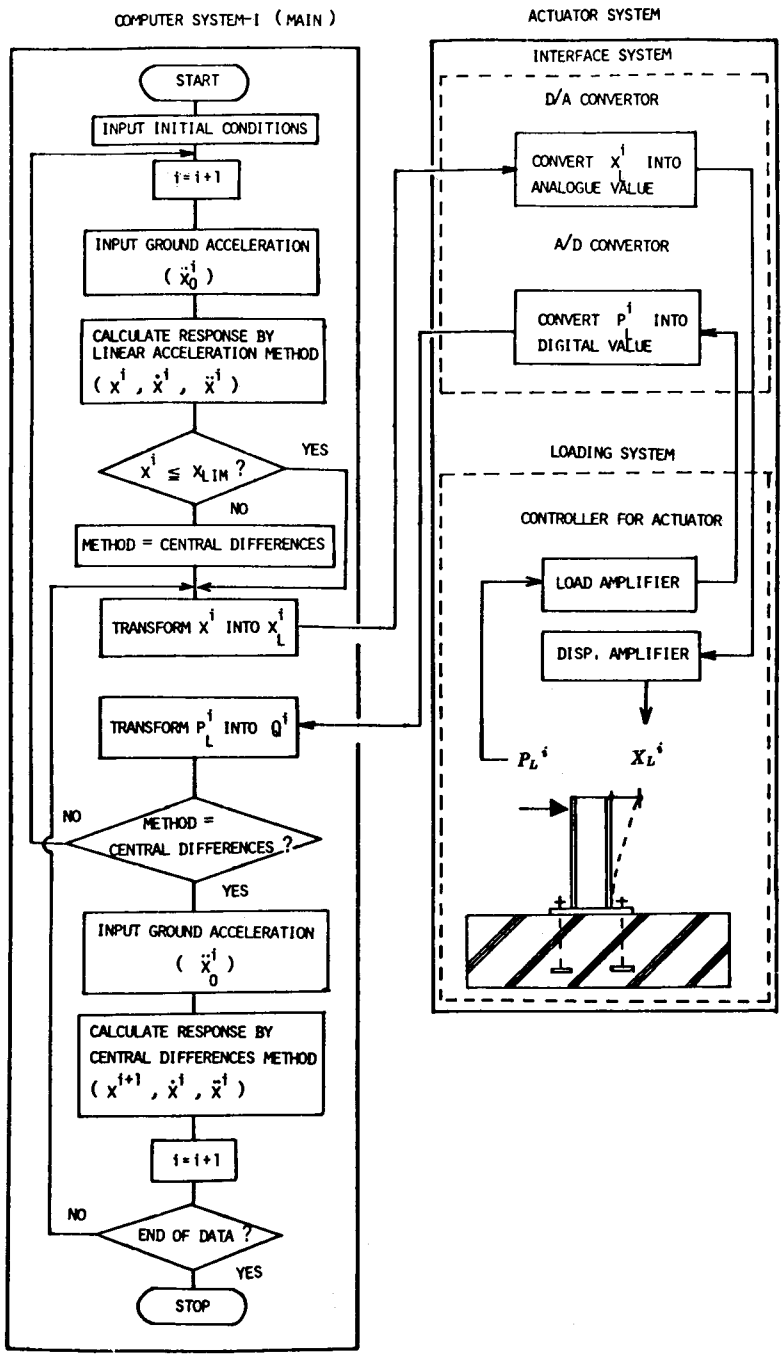

Fig.1.2 Flow diagram of IIS Computer-Actuator On-line System

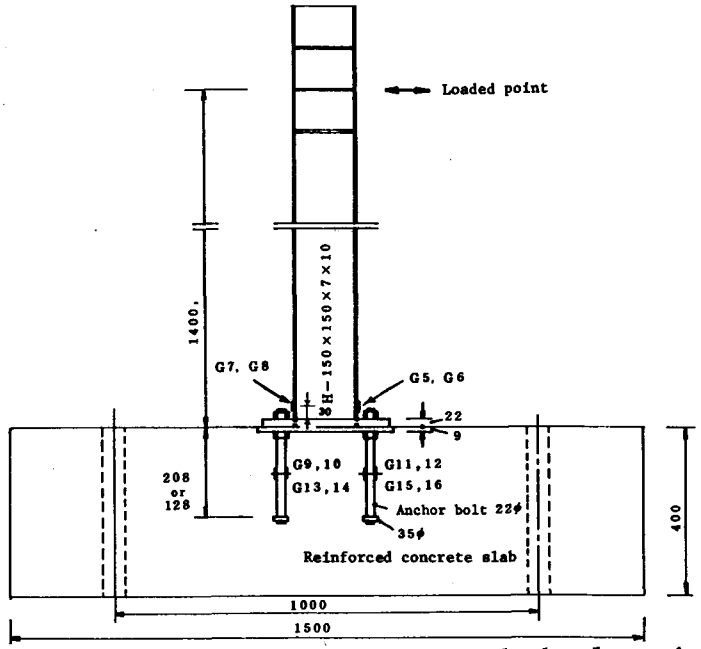

(a) Section of the test structure and the locations of electrical-registance gages

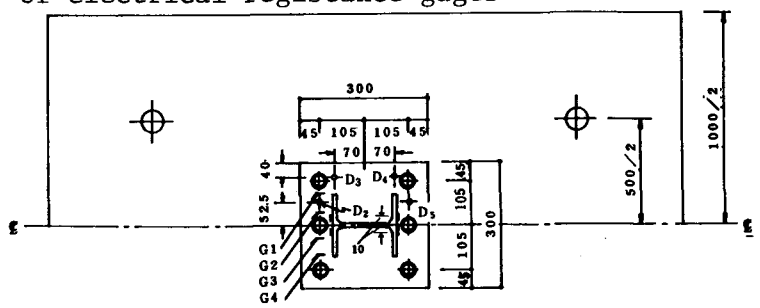

(b) Details of the column base, the locations of gages and displacement meters

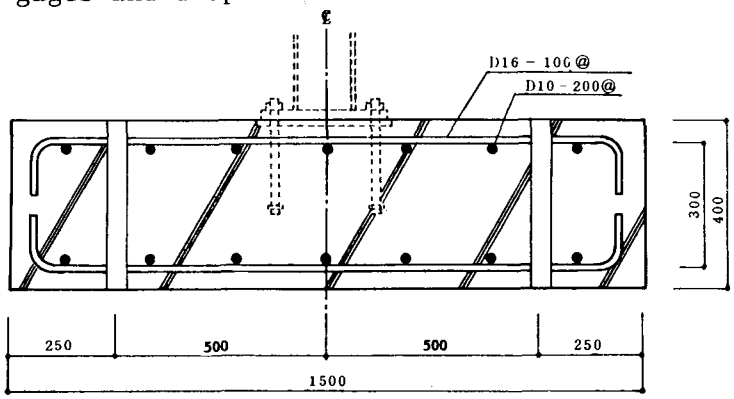

(c) Detail of bar arrangement

Fig.2.1 Test structure and locations of instruments

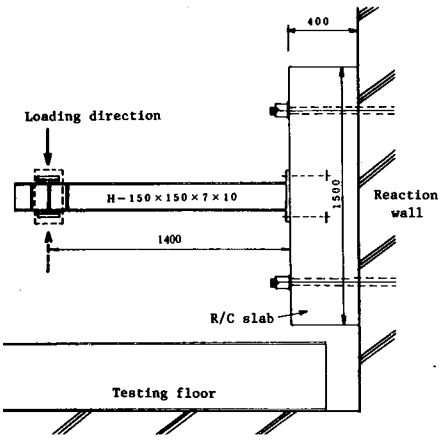

Fig.2.2 Schematic view of test setup

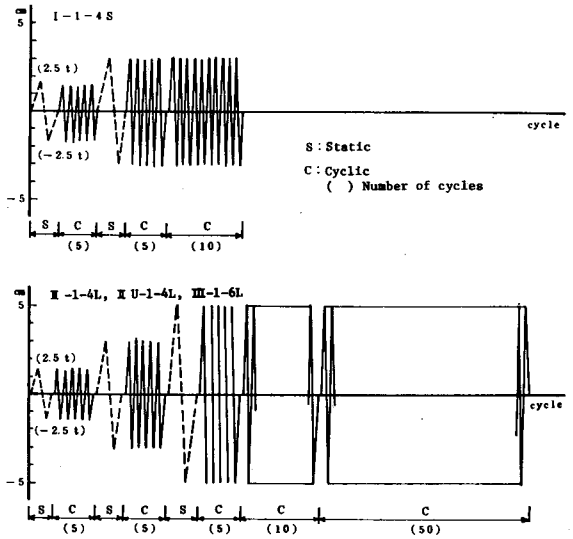

Fig.3.1 Loading programs in cyclic tests

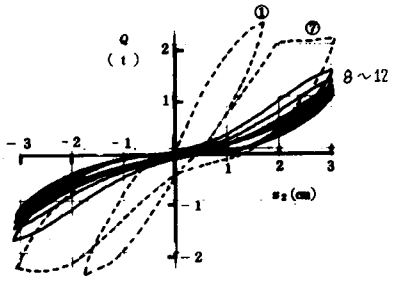

(a) Load-displacement relation (I-1-4S)

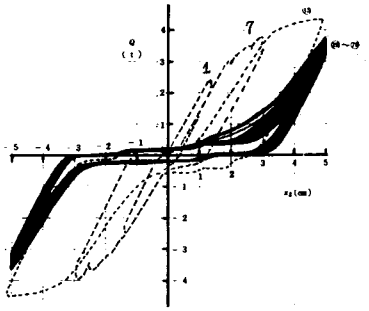

(b) Load-displacement relation (II-1-4L)

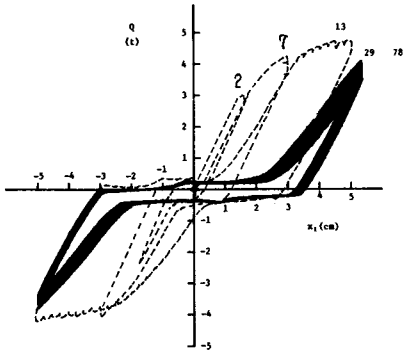

(c) Load-displacement relation (IIU-1-4L)

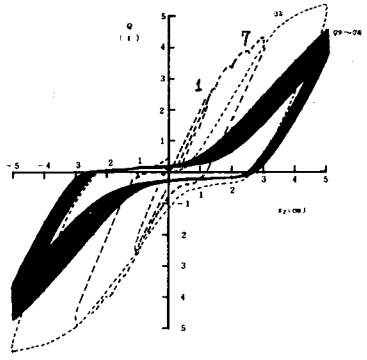

(d) Load-displacement relation (III-1-6L)

Fig.3.2 Lateral load Q vs displacement X_2 relationships

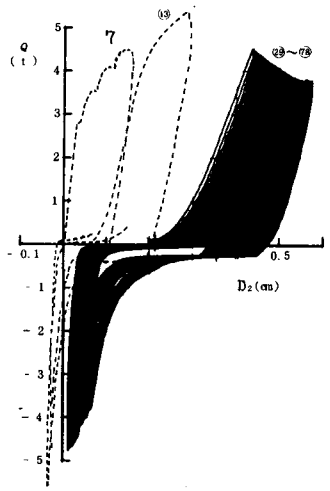

Fig.3.3 Lateral load Q vs uplift displacement D_2

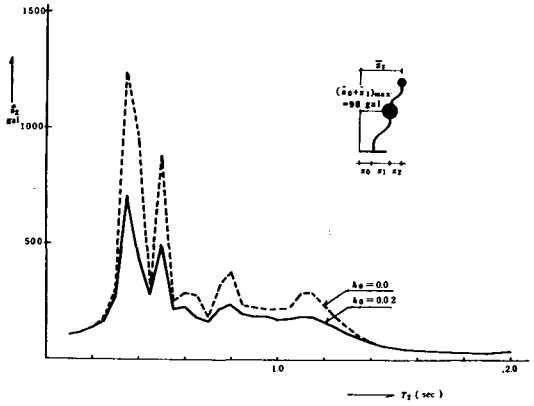

Fig.4.2 Response spectrum of the floor response $[(\ddot{x}_0+\ddot{x}_1)_{max}]$=98 gal

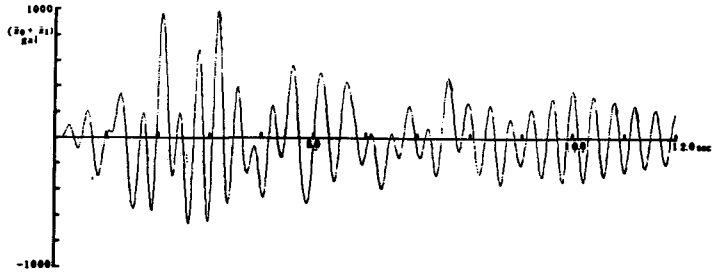

Fig.4.1 Time history of the floor response acceleration used in the simulations $[(\ddot{x}_0+\ddot{x}_1)_{max}]$=980 gal

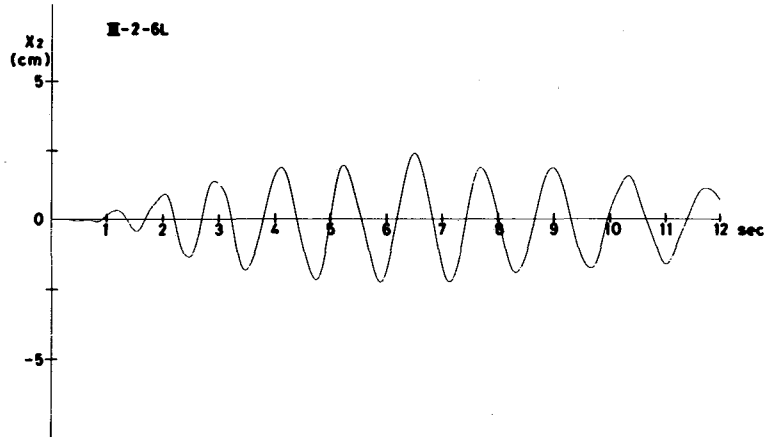

(a) Ⅲ-2-6L (T_0= 0.8 sec)

Fig.4.3 Time histories of response displacements (cont'd)

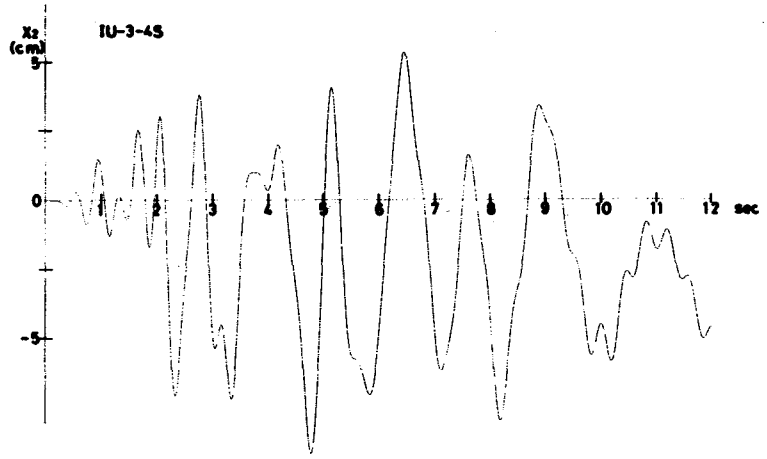

(b) IU-3-4S (T_0 = 0.3 sec)

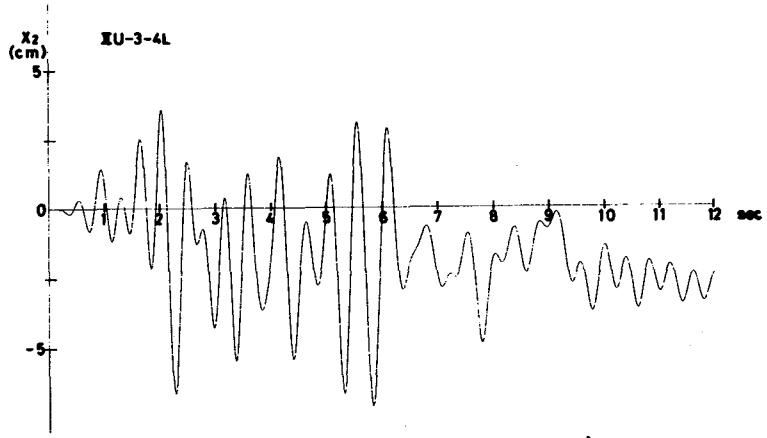

(c) IIU-3-4L (T_0 = 0.3 sec)

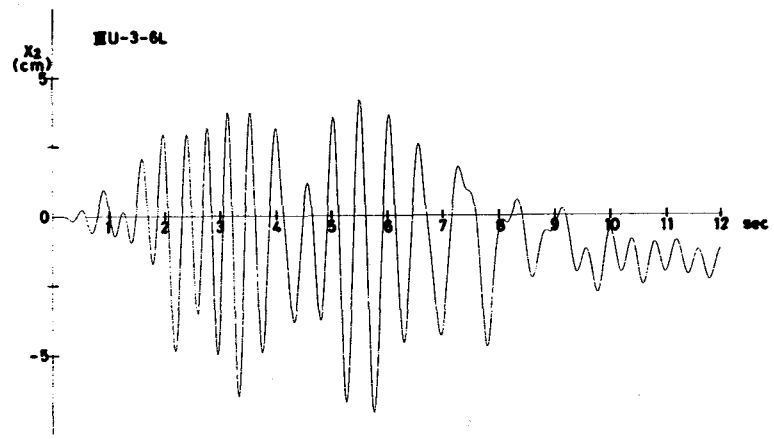

(d) IIIU-3-6L (T_0 = 0.3 sec)

Fig.4.3 Time histories of response displacements

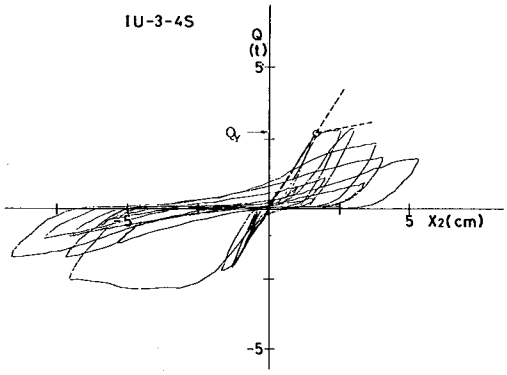

(a) IU-3-4S (T_0 = 0.3 sec)

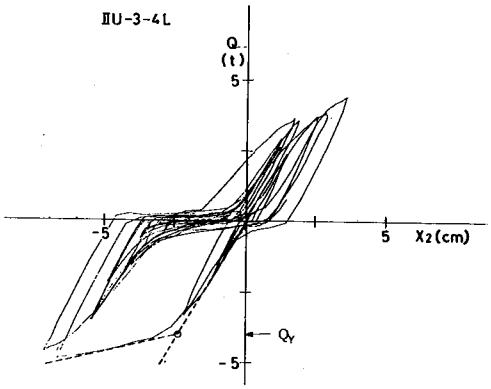

(b) IIU-3-4L (T_0 = 0.3 sec)

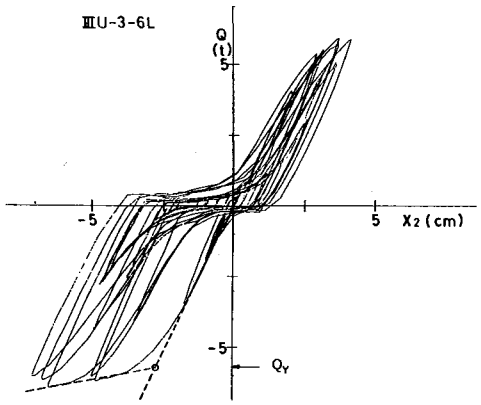

(c) IIIU-3-6L (T_0 = 0.3 sec)

Fig.4.4 Response shear force vs displacement diagrams and yield strength observed

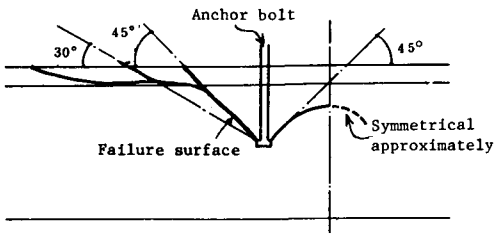

Fig.5.1 Schematic view of the pull out failure mechanism

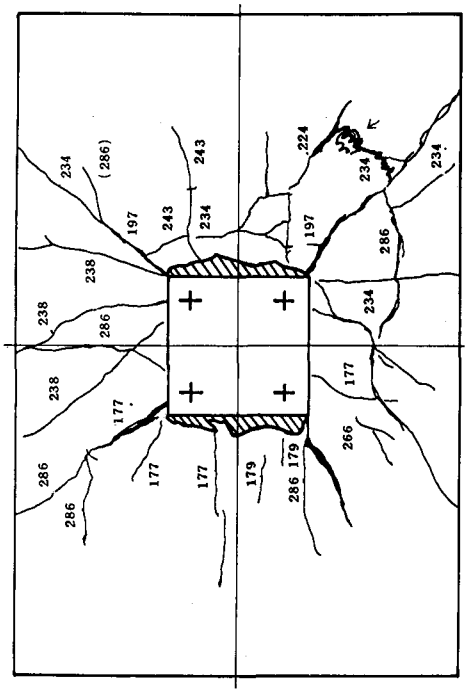

Fig.5.2 Sketch of the cracks on the slab surface caused by pull out failure (IU-3-4S)

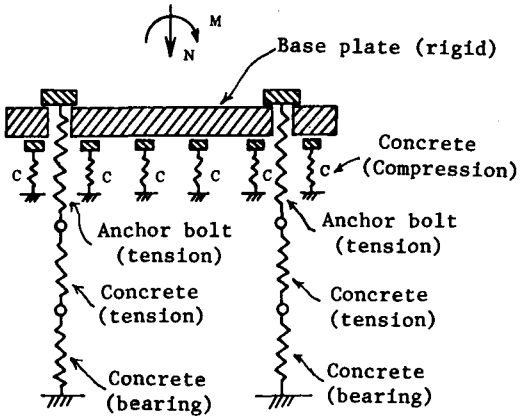

(a) An analytical model

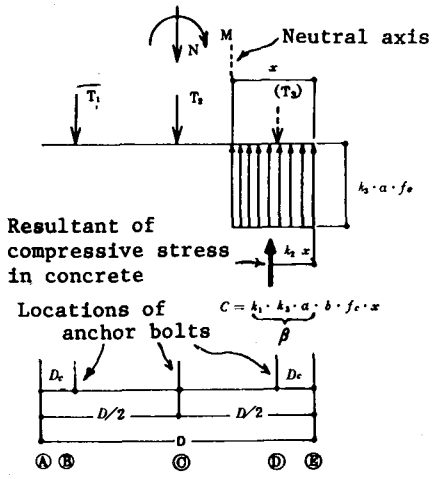

(b) Forces and stress distribution assumed

Fig.5.3 Analytical model and forces and distributed stress acting on the column base

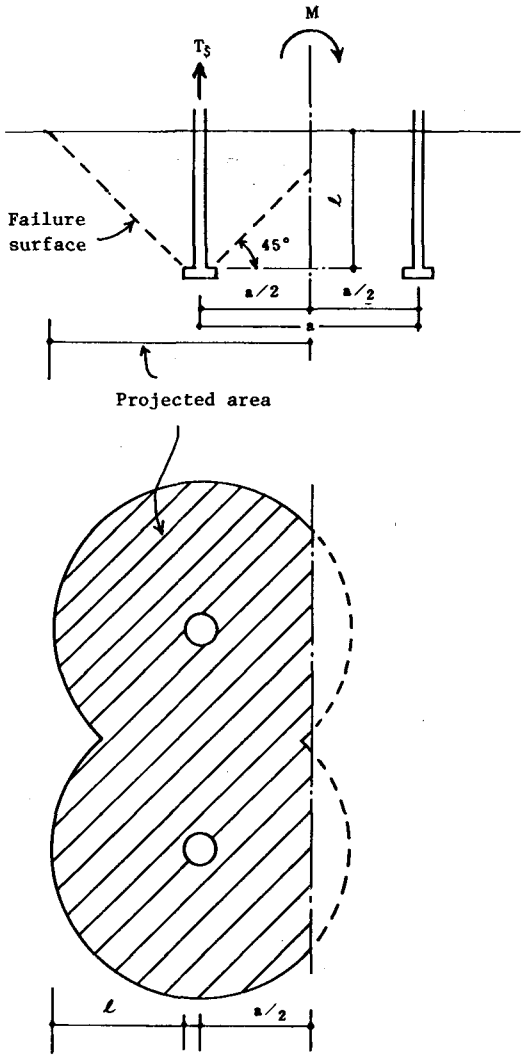

Fig.5.4 Failure surface and its projected area assumed in calculating the pull out failure strength

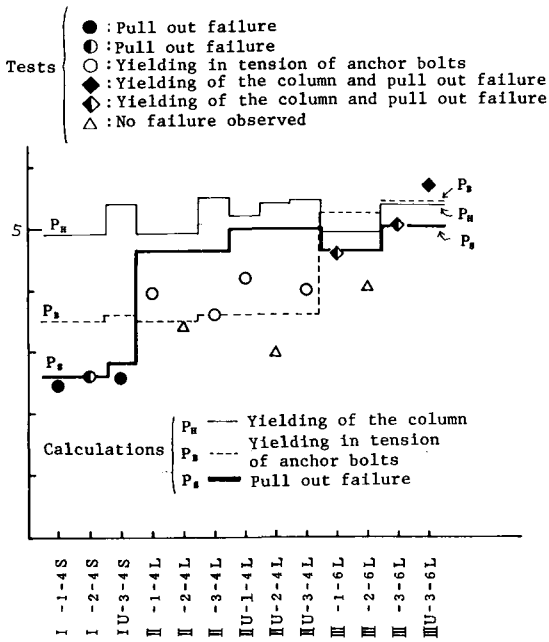

Fig.5.5 Yield strength observed and calculated

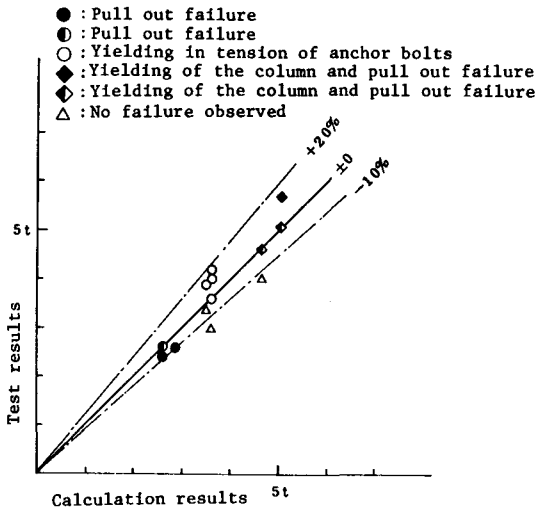

Fig.5.6 Comparison in yield strength observed and calculated

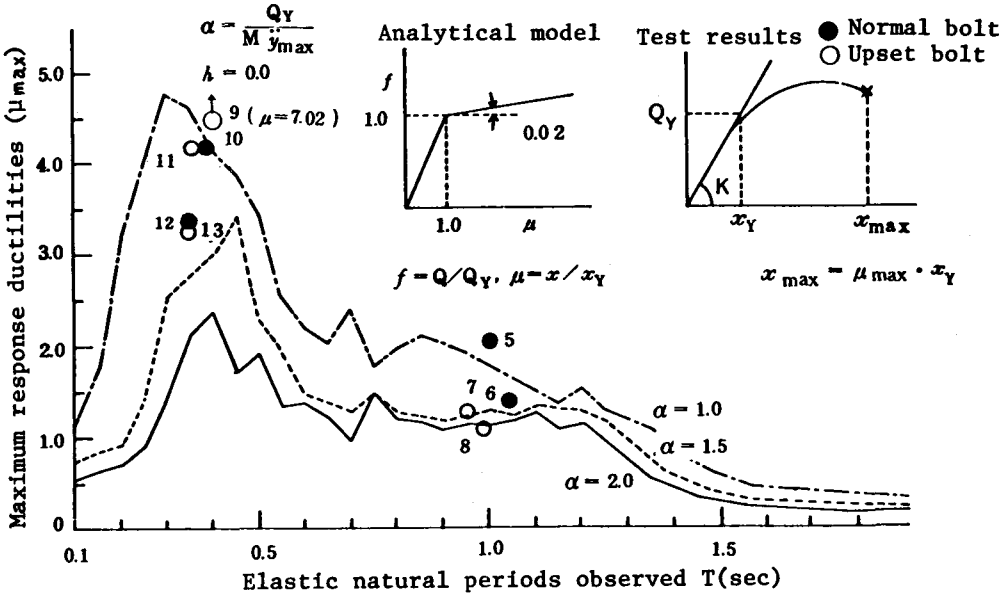

Fig.6.1 Maximum response ductilities

Table 2.1 Test structures and test results

No.		Periods		Specimen code	Anchor bolts		Maximum displacement x_{max} cm	Yield strength Q_Y * ton	Maximum strength Q_{max} ton	Q_{max}/Q_Y	Dominant failure** mechanism observed
		Nominal	Measured		n	Length (mm)					
1	Cyclic test			I -1-4S	4	128 (5.8d)	+3.0 -3.1	2.4	+2.5 -2.3	+1.04 -0.96	Type-S
2				II -1-4L	4	208 (9.5d)	+5.0 -5.0	3.9	+4.3 -4.5	+1.10 -1.15	Type-B
3				II U-1-4L	4	208 (9.5d)	+5.1 -5.1	4.2	+4.2 -4.7	+1.00 -1.12	Type-B
4				III -1-6L	6	208 (9.5d)	+5.1 -5.0	4.6	+5.3 -5.6	+1.15 -1.22	Type-H
5	On-line test	T =0.8 (sec)	1.01	I -2-4S	4	128 (5.8d)	2.38 (4.92sec)	2.6	2.69	1.03	
6			1.04	II -2-4L	4	208 (9.5d)	2.38 (4.84sec)	—	3.40	—	
7			0.95	II U-2-4L	4	208 (9.5d)	2.03 (4.90sec)	—	2.96	—	
8			0.98	III -2-6L	6	208 (9.5d)	2.36 (6.52sec)	—	4.02	—	
9		T =0.3 (sec)	0.40	I U-3-4S	4	128 (5.8d)	9.20 (4.80sec)	2.6	2.90 (2.07sec)	1.12	Type-S
10			0.41	II -3-4L	4	208 (9.5d)	7.54 (5.84sec)	3.6	4.65 (4.80sec)	1.29	Type-B
11			0.37	II U-3-4L	4	208 (9.5d)	7.18 (5.84sec)	4.0	4.94 (2.27sec)	1.24	Type-B
12			0.35	III -3-6L	6	208 (9.5d)	6.58 (3.35sec)	5.1	6.22 (6.28sec)	1.22	Type-H
13			0.35	III U-3-6L	6	208 (9.5d)	7.08 (5.78sec)	5.7	6.45 (3.32sec)	1.13	Type-H and -S

* See Fig.4.4, ** See section 5.1

Table 2.2 Material properties

Test structures	Columns	Anchor bolts		Footing concrete	
	Yield strength	Yield strength	Tensile strength	Compressive strength	Tensile spliting strength
I-1-4S, I-2-4S II-1-4L, II-2-4L III-1-6L, III-2-6L	Flange σ_{YF}=2.80t/cm^2		11.7ton	218.2kg/cm^2	21.22kg/cm^2
II-3-4L, III-3-6L	Web σ_{YW}=2.95t/cm^2	12.1ton	14.9ton	254.2kg/cm^2	22.30kg/cm^2
IIU-1-4L, IU-3-4S IIU-2-4L, IIU-3-4L IIIU-3-6L		12.1ton	18.2ton		

Table 4.1 Simulation results by IIS Computer-Actuator On-line System

No.	Specimen code	Nominal values *1					Measured values				Max. response displacements		Max. response shear forces			
		M t·sec^2/cm	K_o t/cm	T_o sec	Q_{Yo} t	α_o	K *2 t/cm	T *3 sec	Q_Y *4 t	x_Y *5 cm	x_{max} cm	x_{max}/x_Y	Q_{max} t	Q_{max}/Q_Y	Q_{max}/Q_{Yo}	α
5	I -2-4S	.0574	3.54	0.8	4.93	1.87	2.22	1.01	2.6	1.17	2.38	2.03	2.69	1.03	0.546	0.99
6	II -2-4L	.0574	3.54	0.8	4.93	1.87	2.09	1.04	(3.6) *	1.72	2.38	1.38	3.40	0.94	0.690	1.4
7	IIU-2-4L	.0574	3.54	0.8	4.93	1.87	2.51	0.95	(4.0) **	1.59	2.03	1.27	2.96	0.74	0.600	1.5
8	III -2-6L	.0574	3.54	0.8	4.93	1.87	2.36	0.98	(5.1)***	2.16	2.36	1.09	4.02	0.79	0.815	1.9
9	I U-3-4S	.00807	3.54	0.3	4.93	1.87	1.99	0.40	2.6	1.31	9.20	7.02	2.90	1.12	0.588	0.99
10	II -3-4L	.00807	3.54	0.3	4.93	1.87	1.99	0.41	3.6 *	1.81	7.54	4.17	4.65	1.29	0.943	1.4
11	IIU-3-4L	.00807	3.54	0.3	4.93	1.87	2.33	0.37	4.0 **	1.72	7.18	4.18	4.94	1.24	1.00	1.5
12	III -3-6L	.00807	3.54	0.3	4.93	1.87	2.60	0.35	5.1 ***	1.96	6.58	3.36	6.22	1.22	1.26	1.9
13	IIIU-3-6L	.00807	3.54	0.3	4.93	1.87	2.60	0.35	5.7	2.19	7.08	3.23	6.45	1.13	1.31	2.2

*1 cf.4.1, *2 Elastic rigidity measured at Q-x_2 curves, *3 $T=2\pi\sqrt{M/K}$
*4 Yield strength measured at Q-x_2 curves, *5 $x_Y=Q_Y/K$,
*, **, ***( ) denote the same values as the corresponding one

Table 5.1 Results of tests and calculations

	Specimen codes	Anchor bolts		Results of test			Results of calculation				Failure mechanisms observed
		n	Length (mm)	Q_Y ton	Q_{max} ton	$\frac{Q_{max}}{Q_Y}$	P_H ton	P_B *1 ton	P_S *2 ton	P_C ton	
Cyclic test	I -1-4S	4	128 (5.8d)	2.4	2.40	1.00	4.93	4.06	3.09 (3.99)	4.24	Type-S
	II -1-4L	4	208 (9.5d)	3.9	4.40	1.13	4.93	4.06	5.28 (6.77)	5.54	Type-B
	II U-1-4L	4	208 (9.5d)	4.2	4.45	1.06	5.24	4.22 (6.20)	5.74 (7.19)	6.44	Type-B
	III -1-6L	6	208 (9.5d)	4.6	5.45	1.18	4.93	5.93	5.30 (6.80)	6.67	Type-H
On-line test	I -2-4S	4	128 (5.8d)	2.6	2.69	1.03	4.93	4.06	3.09 (3.99)	4.24	
	II -2-4L	4	208 (9.5d)	—	3.40	--	4.93	4.06	5.28 (6.77)	5.54	
	II U-2-4L	4	208 (9.5d)	—	2.96	—	5.43	4.22 (6.20)	5.74 (7.19)	6.44	
	III -2-6L	6	208 (9.5d)	—	4.02	—	4.93	5.93	5.30 (6.80)	6.67	
	I U-3-4S	4	128 (5.8d)	2.6	2.90	1.12	5.43	4.22 (6.20)	3.51 (4.22)	4.93	Type-S
	II -3-4L	4	208 (9.5d)	3.6	4.65	1.29	5.53	4.22 (5.14)	5.74 (7.19)	6.44	Type-B
	II U-3-4L	4	208 (9.5d)	4.0	4.94	1.24	5.49	4.22 (6.20)	5.74 (7.19)	6.44	Type-B
	III -3-6L	6	208 (9.5d)	5.1	6.22	1.22	5.40	6.19 (7.50)	5.76 (7.22)	7.06	Type-H
	IIIU-3-6L	6	208 (9.5d)	5.7	6.45	1.13	5.41	6.19 (8.98)	5.76 (7.22)	7.06	Type-H and -S

*1 The values in ( ) were calculated by tensile stress

*2 $f_s=1.1\sqrt{f_c}$ was used, The values in ( ) were calculated by f_t.